Hydrodynamic separation of colloidal particles in tubes: Effective one-dimensional approach

František Slanina[1,*] and Pavol Kalinay[2]
[1]*Institute of Physics, Academy of Sciences of the Czech Republic, Na Slovance 2, CZ-18221 Praha, Czech Republic*
[2]*Institute of Physics, Slovak Academy of Sciences, Dúbravska cesta 9, 84511, Bratislava, Slovakia*

(Received 3 July 2019; published 9 September 2019)

We investigate diffusion of colloidal particles carried by flow in tubes of variable diameter and under the influence of an external field. We generalize the method mapping the three-dimensional confined diffusion onto an effective one-dimensional problem to the case of nonconservative forces and use this mapping for the problem in question. We show that in the presence of hydrodynamic drag, the lowest approximation (the Fick-Jacobs approximation) may be insufficient, and inclusion of at least the first-order correction is desirable to obtain more reliable results. As a practical application, we use the method for investigation of separation of colloidal particles carried by a fluid flow according to their size, using flotation and centrifugation.

DOI: 10.1103/PhysRevE.100.032606

I. INTRODUCTION

When dealing with colloidal particles suspended in a fluid, we frequently face the problem of sorting them according to their physical properties, like density, size, shape, surface charge, or chirality [1–6]. A natural choice is to use a microfluidic equipment [7–9], where colloids flow through complex geometries, including channels, tubes, arrays of obstacles, and others. The sorting is then achieved by the interplay of hydrodynamic forces, diffusion, and external forces.

External forces typically include gravity, electric and magnetic fields, or centrifugal forces, if the equipment is set into rotation [6]. In a free space, or at least in a large container, hydrodynamic forces acting on a colloid particle are relatively easy to understand, as they include essentially just the Stokes drag, with a correction proportional to the second spatial derivative of the velocity field of the carrying fluid [10]. However, in confined geometry of the microfluidic apparatus, inertial effects and hydrodynamic interactions with walls play an important role. A prominent example is the Segre-Silberberg effect [11–13], which is often used for inertial segregation of particles, with applications, e.g., in blood filtration [14–20]. In this method, channels and tubes of various curved shapes and contraction-expansion arrays are used [21–23]. In a series of papers, we showed how the inertial hydrodynamic effects can be applied to form a hydrodynamic ratchet [24,25]. In this setting, colloidal suspension flows through a tube of periodically varying diameter. Direction of flow is also periodically altered, so that the net flow of the fluid is zero. However, the movement of the colloids is rectified, and their average velocity strongly depends on their size. Experimental realization of deterministic microfluidic ratchets was shown, e.g., in Ref. [26]. Another widely used method of hydrodynamic sorting is the deterministic lateral displacement method [27]. Here the flow goes through a two-dimensional (2D) array of obstacles or through optical [28] or acoustical [29] latices.

For submicrometer particles, Brownian motion plays a decisive role, besides hydrodynamics. Sorting of particles by a combination of diffusion and hydrodynamics was demonstrated in the classical experiment [30], which was modeled theoretically in Ref. [31] and reexamined in Refs. [32,33]. This is closely related to the mechanism of entropic ratchets, which was widely studied [33–41]. In reality, hydrodynamic effects are always present in practical realizations of entropic ratchets, and it was shown that interplay of hydrodynamics and Brownian motion leads to new phenomena, e.g., the hydrodynamically enforced entropic trapping [42,43].

In this paper, we investigate the diffusion of a small particle carried by an incompressible fluid in a tube. The tube is axially symmetric, but its diameter may change along the axis. Moreover, the particle will be exposed to an external field, which may be either uniform and parallel to the axis, or centrifugal, corresponding to rotation of the whole device around the axis. The approach we apply relies on a mapping of three-dimensional (3D) problem to effective one-dimensional (1D) one. There has been much work done on such a mapping procedure, starting from the pioneering works of Jacobs and Zwanzig [44,45] for the diffusion alone. Intuitively, it relies on the following simple idea. If the typical scale of the problem is much smaller in the transverse direction than in the longitudinal one, we can assume that at each place and time the system is equilibrated in the transverse direction, while it may not be equilibrated (or it may be even strongly time-dependent) in general [46,47]. In this way we obtain a 1D equation for probability density projected onto the longitudinal coordinate. This idea was formalized by several procedures [45,46,48–59], which are equivalent in principle but differ in details and in their efficiency. Apart from approximations based on physical insight [46,47] or advanced use of curvilinear coordinates [49,60–63] the mapping methods are mostly based on expansion in a formal small parameter ϵ, which may be interpreted either as the ratio of the longitudinal-to-transverse diffusion constant, transverse length scaling factor, or factor

*slanina@fzu.cz

controlling the amplitude or rate of changes of the tube diameter.

The theory was first developed for diffusion alone [48,64,65]. At zeroth order in the small parameter ϵ the effective 1D Fick-Jacobs (FJ) equation [44] has the form of the Smoluchowski equation for diffusion in an effective potential representing just the entropic contribution from the width of the channel. Higher order terms in ϵ can be found recursively, and the resulting equation of a rather complicated structure can be brought again into the form of the Smoluchowski equation in the limit of stationary flow, but with an effective diffusion coefficient depending on position [65–67]. Approximate formulas for the effective diffusion coefficient were found based on truncated power series [45], general physical arguments [46], or partial resummation of the power series in ϵ [65].

The theory was more or less straightforwardly generalized to the case of conservative external forces, either longitudinal [68–71] or transverse [72], or placing the diffusing particle into a confining potential [73], thus defining "soft walls" of the channel. Time-dependent forces were also studied [40,74].

Nonconservative forces, like hydrodynamic drag, are technically more challenging. There is no scalar potential, and direct application of techniques used for pure diffusion and conservative forces does not lead to an equation of Smoluchowski form even in the zeroth approximation. Enhancement of the longitudinal diffusion of particles advected by a Poisseuille flow in straight channels, known as Taylor dispersion, has been studied for a long time [75,76]. The leading correction to the FJ equation due to the hydrodynamic drag was recently approved also for channels of variable and time-dependent width [77].

One possibility to deal with the general type of driving, including hydrodynamic drag, is to separate the forces into conservative (rotation-free) and nonconservative (divergence-free) components and treat these components with two different procedures. This approach was used successfully [42] and led to the discovery of important effects, like hydrodynamically enforced entropic trapping [42,43,78,79]. However, we encountered situations [80] where the distinction between conservative an nonconservative forces is not possible or, more precisely, is ambiguous. Indeed, if we consider driven diffusion only in a compact area delimited by hard walls, we may partition the force into a rotation-free and divergence-free part in many equivalent ways, just by placing effective charges *outside* the area in question. (This would not be possible if we took into account the entire Euclidean space, as is the case of classical electrodynamics.) Transition from one partitioning to another one can be described by a kind of gauge transform. We used the freedom of the choice of the gauge and developed a general approach for mapping diffusion problems with both conservative and nonconservative forces onto a 1D problem [81]. We choose the gauge explicitly in such a way that the resulting equation again has the Smoluchowski form in the zeroth-order approximation, and the higher order corrections have a form which is suitable for definition of an effective position-dependent diffusion coefficient, as it is routinely used in the case of diffusion alone. We formulated the general method [81] in a 2D setting and applied it to the 2D problem of a Feynmann-Smoluchowski ratchet [80]. Here we rewrite the method for the case of axially symmetric 3D geometry and apply it for several problems connected with the construction of particle-separation devices. The main point is to study the influence of corrugation of the tube on the separation methods, e.g., flotation. In fact, when dealing with hydrodynamic problems, we are forced to work in three dimensions, because true 2D hydrodynamics is to certain extent unphysical. On the other hand, just as a technical remark, we note that axially symmetric 3D problems bring certain simplifications, rather than complications, compared to truly two-dimensional problems.

In Sec. II we outline the general theory of mapping of the confined 3D diffusion driven by a nonconservative force. As an example of practical application of the method developed here we shall investigate separation of particles in tubes with sinusoidally varying diameter in Sec. III. Nevertheless, let us emphasize that the method is completely general, and it can also describe many other situations.

II. GENERALIZED FICK-JACOBS MAPPING IN THREE DIMENSIONS

A. General theory

1. Exact expression

We investigate diffusion of a particle suspended in a fluid in an axially symmetric tube under the influence of external driving. The driving may be of an arbitrary type, including hydrodynamic, electrostatic, magnetic, gravitational, etc. Generally, there is no scalar potential which would correspond to the driving force. We describe the system by cylindric coordinates (x, r, ϕ), where the axis x coincides with the symmetry axis of the tube. All quantities of interest will be assumed independent of the angle ϕ; therefore, the problem is effectively 2D. This does not mean that the velocity of the fluid in the tube does not have an angular component; we just assume that the probability density for the position of the particle is independent of ϕ.

We assume that the tube has hard walls and the radius of the tube changes along the axis according to a function $h(x)$. In the applications we show later the function $h(x)$ will be periodic, but the general formalism holds for any analytic function $h(x)$. The diffusing particle is subject to a driving force which can be decomposed into an axial and radial component, described by functions $F_x(x, r)$ and $F_r(x, r)$, respectively. The primary quantity of interest is the probability density for the particle $\rho(x, r, t)$ obeying the general advection-diffusion equation

$$\partial_t \rho(x,r,t) = D_0 \left\{ \partial_x [\partial_x - \beta F_x(x,r)] + \frac{1}{r} \partial_r r [\partial_r - \beta F_r(x,r)] \right\} \times \rho(x,r,t), \tag{1}$$

where D_0 denotes the intrinsic diffusion constant, and $\beta = 1/k_B T$ is the inverse temperature. Here and in the rest of the article we denote ∂_t, ∂_x, ∂_r partial derivatives with respect to time, with respect to x with r fixed and with respect of r with x fixed, respectively. However, the method of solution will consist mainly in projecting this density on the axis. So in the

1D picture, we shall work with the projected density

$$p(x,t) = \int_0^{h(x)} 2\pi r \rho(x,r,t)\, dr. \tag{2}$$

The key point of the mapping procedure is scaling of the transverse lengths r, $h(x)$ by a small parameter $\sqrt{\epsilon}$ and, correspondingly, the transverse component of force $F_r(x,r)$ by $1/\sqrt{\epsilon}$. We shall obtain the approximate equations for $p(x,t)$ in terms of the series in powers of ϵ, which describes separation of timescales for the movement in radial, compared to axial, directions. Applying the scaling, we obtain our starting equation in the form

$$\partial_t \rho(x,r,t) = \partial_x[\partial_x - f(x,r)]\rho(x,r,t) + \frac{1}{\epsilon r}\partial_r\, r[\partial_r - g(x,r)]\rho(x,r,t). \tag{3}$$

We have introduced here the reduced parameters $f(x,r) = \beta F_x(x,r)$, $g(x,r) = \beta F_r(x,r)$, and the time is rescaled by the diffusion constant, $D_0 t \to t$.

Finally, Eq. (3) is supplemented by the boundary conditions (BCs):

$$\begin{aligned} &\{[\partial_r - g(x,r)]\rho(x,r,t)\}_{r=0} = 0 \quad \forall x \forall t \\ &\{[\partial_r - g(x,r)]\rho(x,r,t)\}_{r=h(x)} \\ &\quad = \epsilon h'(x)\{[\partial_x - f(x,r)]\}]_{r=h(x)} \quad \forall x \forall t. \end{aligned} \tag{4}$$

Integrating (3) over the cross section and using (4), we get an exact equation for the projected density, namely,

$$\partial_t p(x,t) = \partial_x^2 p(x,t) - \partial_x[2\pi h'(x)h(x)\rho(x,h(x),t)] - \partial_x \int_0^{h(x)} 2\pi r f(x,r)\rho(x,r,t)\, dr. \tag{5}$$

Our task now is to express $\rho(x,r,t)$ using $p(x,t)$ to find the mapped equation for the projected density in a closed form.

2. Series expansion

For the conservative forces, $(F_x, F_r) = -\nabla U(x,r)$, where the corresponding scalar potential $U(x,r)$ exists, we obtain the 1D equation of the Smoluchowski form

$$\partial_t p(x,t) = \partial_x A(x)\partial_x \frac{p(x,t)}{A(x)} \tag{6}$$

in the zeroth order in ϵ, supposing instantaneous equilibration in the transverse direction. The function $A(x) = \int_0^{h(x)} 2\pi r e^{-\beta U(x,r)} dr$ is related to the effective 1D potential in which the particle moves. The mapping procedure generates corrections to this equation in the higher orders,

$$\partial_t p(x,t) = \partial_x A(x)[1 - \widehat{Z}(x,\partial_x)]\partial_x \frac{p(x,t)}{A(x)}, \tag{7}$$

where the operator $\widehat{Z}(x,\partial_x)$ is expressed as power series in the parameter ϵ,

$$\widehat{Z}(x,\partial_x) = \sum_{k=1}^{\infty} \epsilon^k \widehat{Z}_k(x,\partial_x). \tag{8}$$

We showed in our previous work [80,81] that in the 2D case it is possible to find the equation for $p(x,t)$ in the same form, having redefined the function $A(x)$. We extend validity of such an equation for the 3D case here, skipping details which are literally identical to two dimensions.

An analysis [81] applied for 3D channels shows that for nonconservative forces as well there can be defined a function

$$G(x,r) = G_{00}(x,r) - \gamma(x) \tag{9}$$

which plays the role of the scalar potential in our mapping formalism. Here

$$G_{00}(x,r) = -\int_0^r g(x,r')\, dr' \tag{10}$$

and $\gamma(x)$ is a gauge function which will be discussed later. In order to obtain (7) from (5) we need a kind of backward projection from the function $p(x,t)$ to the density $\rho(x,r,t)$. Following arguments in Ref. [81], we assume the following ansatz for this projection:

$$\rho(x,r,t) = e^{-G(x,r)}[1 + \widehat{\omega}(x,r,\partial_x)]\frac{p(x,t)}{A(x)}; \tag{11}$$

the entropic factor $A(x)$ is redefined as

$$A(x) = \int_0^{h(x)} 2\pi r\, e^{-G(x,r)}\, dr. \tag{12}$$

Still, the operator of backward mapping $\widehat{\omega}(x,r,\partial_x)$ and the gauge function $\gamma(x)$ in $G(x,r)$ and $A(x)$ are to be determined. Similarly to (8), the operator $\widehat{\omega}(x,r,\partial_x)$ also can be expressed as a power series in ϵ:

$$\widehat{\omega}(x,r,\partial_x) = \sum_{k=1}^{\infty} \epsilon^k \widehat{\omega}_k(x,r,\partial_x). \tag{13}$$

The successive terms $\widehat{\omega}_1$, $\widehat{\omega}_2$, etc., can be obtained iteratively, substituting the backward projection (11) into the original advection-diffusion equation (3) and comparing terms at the same power of ϵ [81]. For example, for the leading correction $\widehat{\omega}_1$ we obtain a differential equation of the following form:

$$\frac{1}{r}\partial_r r\, e^{-G_{00}(x,r)}\, \partial_r \widehat{\omega}_1(x,r,\partial_x) = e^{-G_{00}(x,r)}\big[T_1^I(x,r) + T_1^{II}(x,r)\partial_x\big]. \tag{14}$$

The functions $T_1^I(x,r)$ and $T_1^{II}(x,r)$ will be shown explicitly later. Both sides of these equations are understood as operators acting on any function of x.

From the form of Eq. (14) it is clear that the operator $\widehat{\omega}_1$ can be partitioned into two terms

$$\widehat{\omega}_1(x,r,\partial_x) = \omega_1^I(x,r) + \omega_1^{II}(x,r)\partial_x, \tag{15}$$

where $\omega_1^I(x,r)$ and $\omega_1^{II}(x,r)$ are just functions of x and r, not containing the differentiation operator. It can be shown that analogous property holds to all orders in ϵ, so that the entire operator $\widehat{\omega}$ can be partitioned as

$$\widehat{\omega}(x,r,\partial_x) = \omega^I(x,r) + \widehat{\omega}^{II}(x,r,\partial_x)\partial_x, \tag{16}$$

where now $\omega^I(x,r)$ is just a function of x and r, while $\widehat{\omega}^{II}(x,r,\partial_x)$ is an operator, which may in general also contain the partial derivative ∂_x. This partitioning is essential for fixing the gauge term $\gamma(x)$. For conservative forces, $\omega^I(x,r) = 0$, and the projection technique results directly in Eq. (7). For nonconservative forces, contributions from nonzero $\omega^I(x,r)$

have to be eliminated by the proper choice of $\gamma(x)$ to bring the mapped equation to the form of (7).

First, we assume that this function is also expanded into power series in ϵ, i.e.,

$$\gamma(x) = \gamma_0(x) + \widetilde{\gamma}(x) = \gamma_0(x) + \sum_{k=1}^{\infty} \epsilon^k \gamma_k(x). \tag{17}$$

In order to formulate the general conditions fixing the terms $\gamma_0(x)$ and $\widetilde{\gamma}(x)$, let us introduce the following notation. For any function (or operator) $F(x,r)$ we define the average with respect to function $G_{00}(x,r)$ as

$$\langle F\rangle(x) = \frac{1}{A_{00}(x)} \int_0^{h(x)} 2\pi r\, F(x,r)\, e^{-G_{00}(x,r)}\, dr, \tag{18}$$

where

$$A_{00}(x) = \int_0^{h(x)} 2\pi r\, e^{-G_{00}(x,r)}\, dr. \tag{19}$$

Note that this average is independent of the choice of gauge. Using this notation, we find that the gauge which brings the equation for $p(x,t)$ into the form (7) should obey the equations

$$\gamma_0'(x) = \langle G_{00}' + f\rangle(x) \tag{20}$$

(the prime denotes partial differentiation with respect to x with r fixed) and

$$\widetilde{\gamma}'(x) = \langle f\omega^I\rangle(x) + \frac{2\pi h'(x)h(x)}{A_{00}(x)} e^{-G_{00}(x,h(x))}\, \omega^I(x,h(x)). \tag{21}$$

With this choice of gauge, the equation for $p(x,t)$ takes the form (7) with the operator $\widehat{Z}$ written explicitly as

$$\widehat{Z}(x,\partial_x) = \langle f\widehat{\omega}^{II}\rangle(x,\partial_x) + \frac{2\pi h'(x)h(x)}{A_{00}(x)} e^{-G_{00}(x,h(x))}\, \widehat{\omega}^{II}(x,h(x),\partial_x). \tag{22}$$

B. Lowest approximations

1. Zeroth order

The expansion in powers of ϵ must be obtained iteratively, step by step. So let us start with the zeroth approximation. Both $\widehat{\omega}$ and $\widehat{Z}$ are zero at this order, but the gauge term already assumes the lowest correction (20). In the backward projection for the density this correction cancels, and in the zeroth order we have

$$\rho_0(x,r,t) = e^{-G_{00}(x,r)} \frac{p_0(x,t)}{A_{00}(x)}. \tag{23}$$

Here $p_0(x,t)$ is the projected density, which is the solution of the equation

$$\partial_t p_0(x,t) = \partial_x A_0(x) \partial_x \frac{p_0(x,t)}{A_0(x)} \tag{24}$$

in which the gauge term enters through the factor $A_0(x) = A_{00}(x)\, e^{\gamma_0(x)}$. In this way the gauge factor influences the backward projected density even in the zeroth approximation.

2. First order

The starting point for the calculation of the corrections to the first order in ϵ is the differential equation for the operator $\widehat{\omega}_1$, which we have already written in (14). The functions $T_1^I(x,r)$ and $T_1^{II}(x,r)$ which occur in Eq. (14) can be found explicitly as

$$\begin{aligned} T_1^I(x,r) &= G_{00}''(x,r) - \langle G_{00}''\rangle(x) + f(x,r) - \langle f\rangle(x) - [G_{00}'(x,r)]^2 + \langle (G_{00}')^2\rangle(x) - f(x,r)G_{00}'(x,r) \\ &\quad + \langle f\, G_{00}'\rangle(x) - [G_{00}'(x,h(x)) - \langle G_{00}'\rangle(x) + f(x,h(x)) - \langle f\rangle(x)] \frac{2\pi h'(x)h(x)}{A_{00}(x)} e^{-G_{00}(x,h(x))} \\ &\quad + [2G_{00}'(x,r) - 2\langle G_{00}'\rangle(x) + f(x,r) - \langle f\rangle(x)][\langle G_{00}'\rangle(x) + \langle f\rangle(x)], \\ T_1^{II}(x,r) &= \frac{2\pi h'(x)h(x)}{A_{00}(x)} \exp[-G_{00}(x,h(x))] + 2G_{00}'(x,r) - 2\langle G_{00}'\rangle(x) + f(x,r) - \langle f\rangle(x). \end{aligned} \tag{25}$$

It is clear from Eq. (14) that the functions $\omega_1^I(x,r)$ and $\omega_1^{II}(x,r)$ depend only on functions $T_1^I(x,r)$ and $T_1^{II}(x,r)$, respectively. Therefore, we can write the solution of (14) in one compact formula,

$$\begin{aligned} \omega_1^\sigma(x,r) &= \int_0^r \frac{1}{r'} e^{G_{00}(x,r')} \int_0^{r'} r''\, e^{-G_{00}(x,r'')}\, T_1^\sigma(x,r'')\, dr''dr' \\ &\quad - \frac{1}{\int_0^{h(x)} r'\, e^{-G_{00}(x,r')}\, dr'} \int_0^{h(x)} r'\, e^{-G_{00}(x,r')} \\ &\quad \times \int_0^{r'} \frac{1}{r''} e^{G_{00}(x,r'')} \int_0^{r''} r'''\, e^{-G_{00}(x,r''')}\, T_1^\sigma(x,r''') \\ &\quad \times dr'''dr''dr', \end{aligned} \tag{26}$$

taking the BC $\partial_r \omega_1^\sigma(x,r)|_{r=0} = 0$ and normalization $\int_0^{h(x)} 2\pi r e^{-G_{00}(x,r)} \omega_1^\sigma(x,r)\, dr = 0$ into account; the upper index assumes the values $\sigma \in \{I, II\}$. With the correction to the backward projector $\widehat{\omega}_1$ at our disposal, we can calculate the next correction to the gauge term

$$\gamma_1'(x) = \langle f\omega_1^I\rangle(x) + \frac{2\pi h'(x)h(x)}{A_{00}(x)} e^{-G_{00}(x,h(x))}\, \omega_1^I(x,h(x)) \tag{27}$$

and the lowest term in the operator $\widehat{Z}$, which is just a function of x in the first order

$$Z_1(x) = \langle f\omega_1^{II}\rangle(x) + \frac{2\pi h'(x)h(x)}{A_{00}(x)} e^{-G_{00}(x,h(x))}\, \omega_1^{II}(x,h(x)). \tag{28}$$

The projected density up to the first order in ϵ, denoted as $p_1(x,t)$, is then the solution of the equation

$$\partial_t p_1(x,t) = \partial_x A_1(x)[1-\epsilon Z_1(x)]\partial_x \frac{p_1(x,t)}{A_1(x)}, \tag{29}$$

where $A_1(x) = A_{00}(x)\, e^{\gamma_0(x)+\epsilon\gamma_1(x)}$ contains the gauge term up to the first order in ϵ. Having solved (29), we can project $p_1(x,t)$ backward to obtain the probability density up to the first order

$$\rho_1(x,r,t) = e^{-G_1(x,r)}\left\{1+\epsilon\left[\omega_1^I(x,r)+\omega_1^{II}(x,r)\partial_x\right]\right\} \times \frac{p_1(x,t)}{A_1(x)}. \tag{30}$$

Here we denoted $G_1(x,r) = G_{00}(x,r) - \gamma_0(x) - \epsilon\gamma_1(x)$, the function $G(x,r)$ approximated up to the first order.

In the following, we shall be also interested in total particle current, incorporating both the drift and diffusion components. The axial and radial components of the current are, by definition,

$$j_x(x,r,t) = (f(x,r)-\partial_x)\rho(x,r,t),$$
$$j_r(x,r,t) = \frac{1}{\epsilon}(g(x,r)-\partial_r)\rho(x,r,t). \tag{31}$$

In all what follows, we limit the discussion to stationary states, so there is no time dependence of the current.

In practical calculation, there is an annoying problem stemming from the fact that the two components of the current defined in (31) are of different order in ϵ. Therefore, in any finite order in ϵ we face the following dilemma. Either the continuity equation

$$\partial_x j_x(x,r,t) + \frac{1}{r}\partial_r r j_r(x,r,t) = 0 \tag{32}$$

is violated, or the two components of the current are not calculated to the same order in ϵ. In this work, we consider satisfaction of the continuity equation too valuable to sacrifice it. Thus, when calculating the current within a given order in ϵ, we start with the backward projected density ρ in this order, calculate j_x from it according to (31), and then complete the task by calculating j_r such that it satisfies (32). In this procedure, a useful auxiliary quantity is the particle stream function defined as

$$\Phi(x,r) = \int_0^r r' j_x(x,r')\, dr'. \tag{33}$$

Then the radial current is simply

$$j_r(x,r) = -\frac{1}{r}\frac{\partial\Phi(x,r)}{\partial x}, \tag{34}$$

and (32) is satisfied automatically.

III. COMBINATION OF FLOW AND EXTERNAL FORCES

A. Pure flow

1. General consideration

We shall investigate diffusion in a flowing liquid in a tube of varying diameter [82]. The problem of fluid flow in such a tube is itself a tricky task [83–86]. Increasing the Reynolds number, various regimes are observed, from a simple vortex-free flow, to nontrivial structure of vortices, to unstable flow, to fully developed turbulence. We shall omit all these delicacies, assuming a negligible value of the Reynolds number [10]. In this regime, the flow is described by the Stokes equation, instead of the full Navier-Stokes equation. However, even the solution of the Stokes equation is far from trivial [87–89]. One of the procedures is the expansion of the solution of the Stokes equation in the amplitude of the variation of the diameter [24,25,90,91]. Here we shall use only the lowest term in this expansion. This is the simplest possible approximation compatible with the geometry of the tube. In fact, it is just geometrically deformed Poisseuille flow. In terms of the Stokes stream function, the drag of flow is, in this approximation, described as

$$\psi(x,r) = \frac{4q}{\pi}\left\{\left[\frac{r}{2h(x)}\right]^2 - 2\left[\frac{r}{2h(x)}\right]^4\right\}, \tag{35}$$

where q is the amplitude of hydrodynamic force, proportional to total volumetric flow through the tube.

When a spherical particle is passively carried by the flow, its velocity can be computed from the velocity field of the fluid. When the flow is described by the Stokes equation, the calculation is relatively easy; the resulting particle velocity is given by the velocity of the fluid in the absence of the particle plus a correction term proportional to the square of the particle diameter. (In the case of Navier-Stokes flow, further corrections come into play.) We suppose that our particles are small enough so that we can neglect the correction term. Therefore, the hydrodynamic drag results in the following driving forces acting on the particle:

$$g(x,r) = -\frac{1}{r}\frac{\partial\psi(x,r)}{\partial x}, \quad f(x,r) = \frac{1}{r}\frac{\partial\psi(x,r)}{\partial r}. \tag{36}$$

Inserting the driving (36) with flow defined as (35) into the general formalism presented in Sec. II, we can finally obtain the probability density for the particle diffusing in a flowing fluid in the absence of any external force.

In this work, we shall be interested only in the stationary state. Therefore, in Eq. (7), as well as in the approximate equations (24) and (29), the left-hand side vanishes. For example, up to the first order in ϵ we obtain for the stationary projected density the solution

$$p_1(x) = A_1(x)\left\{c - \int_0^x \frac{j}{A_1(x')[1-\epsilon Z_1(x')]}\, dx'\right\}, \tag{37}$$

where the integration constant c and the total stationary current j should be determined from the boundary conditions. In the zeroth order, an analogous formula holds, further simplified by the absence of the Z term in the denominator. Taking the higher order corrections in ϵ requires us to replace $1-\epsilon Z_1(x)$ by an effective diffusion coefficient $D(x)$ calculated from the coefficients $\widehat{Z}_n$ in the same way as in Ref. [81].

We can see from (35) that the functions $G_{00}(x,r)$ and $f(x,r)$ which appear in the formalism of Sec. II are polynomials of r^2. This suggests the change of variables $(x,r) \to (x,v)$

according to

$$v = 1 - \frac{r^2}{h^2(x)}. \tag{38}$$

After such a substitution we can write

$$\begin{aligned} G_{00}(x,r) &= \widetilde{G}_{00}(x,v) = \zeta_0(x) + \zeta_1(x)v + \zeta_2(x)v^2, \\ f(x,r) &= \widetilde{f}(x,v) = \eta_0(x) + \eta_1(x)v, \end{aligned} \tag{39}$$

where the information on the shape of the tube is contained in the set of functions $\zeta_\alpha(x)$ and $\eta_\alpha(x)$. The explicit formulas for them are given in the Appendix. Inserting (39) into (25) we obtain

$$\begin{aligned} T_1^I(x,r) &= \widetilde{T}_1^I(x,v) = \sum_{\alpha=0}^{4} T_{1,\alpha}^I(x) v^\alpha, \\ T_1^{II}(x,r) &= \widetilde{T}_1^{II}(x,v) = \sum_{\alpha=0}^{2} T_{1,\alpha}^{II}(x) v^\alpha, \end{aligned} \tag{40}$$

where the set of functions $T_{1,\alpha}^I(x)$ and $T_{1,\alpha}^{II}(x)$ can be expressed through the set of functions $\zeta_\alpha(x)$ and $\eta_\alpha(x)$, and explicit expressions are again given in the Appendix. This formalism allows us to perform the integrations in the formula (26) independently of the actual shape of the tube. Indeed, we can define the following functions of two variables:

$$\begin{aligned} \Lambda(z_1,z_2) &= \int_0^1 e^{-z_1 v - z_2 v^2}\, dv, \\ \Lambda_\beta(z_1,z_2) &= \int_0^1 \frac{1}{1-v'} e^{z_1 v' + z_2 v'^2} \int_{v'}^1 e^{-z_1 v'' - z_2 v''^2}\, v''^\beta\, dv''\, dv', \\ \Lambda_{\alpha\beta}(z_1,z_2) &= \int_0^1 v^\alpha\, e^{-z_1 v - z_2 v^2} \int_v^1 \frac{1}{1-v'} e^{z_1 v' + z_2 v'^2} \int_{v'}^1 e^{-z_1 v'' - z_2 v''^2}\, v''^\beta\, dv''\, dv'\, dv, \\ \langle v^\alpha \rangle(z_1,z_2) &= \frac{1}{\Lambda(z_1,z_2)} \int_0^1 v^\alpha\, e^{-z_1 v - z_2 v^2}\, dv, \\ \Delta_\beta(v;z_1,z_2) &= \int_v^1 \frac{1}{1-v'} e^{z_1 v' + z_2 v'^2} \int_{v'}^1 e^{-z_1 v'' - z_2 v''^2}\, v''^\beta\, dv''\, dv'\, dv. \end{aligned} \tag{41}$$

In fact, not all of them are independent. For example, $\Delta_\beta(0,x_1,z_2) = \Lambda_\beta(z_1,z_2)$. In the Appendix we show how $\langle v^\alpha \rangle(z_1,z_2)$ can be expressed using $\Lambda(z_1,z_2)$. With help of the functions defined in (41) we can write

$$\begin{aligned} \gamma_0'(x) &= \eta_0(x) + \zeta_0'(x) + [\eta_1(x) + \zeta_1'(x)]\langle v \rangle + \zeta_2'(x)\langle v^2 \rangle \\ &\quad + \frac{2h'(x)}{h(x)}\zeta_1(x)(1 - \langle v \rangle) + \frac{4h'(x)}{h(x)}\zeta_2(x)(\langle v \rangle - \langle v^2 \rangle), \end{aligned} \tag{42}$$

and the formulas for $\gamma_1(x)$ and $Z_1(x)$ can be expressed in a compact form:

$$\begin{aligned} \gamma_1'(x) &= \frac{1}{4\Lambda} \sum_{\beta=0}^{4} \left[2h'(x)h(x)\left(\Lambda_\beta - \frac{\Lambda_{0\beta}}{\Lambda}\right) \right. \\ &\quad \left. + h^2(x)\eta_1(x)(\Lambda_{1\beta} - \langle v \rangle \Lambda_{0\beta}) \right] T_{1,\beta}^I(x), \\ Z_1(x) &= \frac{1}{4\Lambda} \sum_{\beta=0}^{2} \left[2h'(x)h(x)\left(\Lambda_\beta - \frac{\Lambda_{0\beta}}{\Lambda}\right) \right. \\ &\quad \left. + h^2(x)\eta_1(x)(\Lambda_{1\beta} - \langle v \rangle \Lambda_{0\beta}) \right] T_{1,\beta}^{II}(x). \end{aligned} \tag{43}$$

In (42) and (43), the functions defined in (41) are written without arguments. Doing that, we intend that the replacement $z_1 \leftarrow \zeta_1(x)$, $z_2 \leftarrow \zeta_2(x)$ is performed everywhere in (42) and (43). We believe that the advantage of this formalism lies in the fact that the calculation of complicated integrals is separated from the choice of geometry.

For backward projection of the density according to (30) we shall also need the functions $\omega_1^\sigma(x,r)$ for $\sigma \in \{I, II\}$. Here we use the same change of variables and write

$$\begin{aligned} \omega_1^\sigma(x,r) &= \widetilde{\omega}_1^\sigma(x,v) \\ &= \frac{h^2(x)}{4} \sum_{\beta=0}^{k_\sigma} \left[\Delta_\beta(v) - \frac{\Lambda_{0\beta}}{\Lambda} \right] T_{1,\beta}^\sigma(x). \end{aligned} \tag{44}$$

Here again, the missing arguments z_1, z_2 are intended to be replaced by $\zeta_1(x)$ and $\zeta_2(x)$, respectively. The upper summation limit is $k_I = 4$ and $k_{II} = 2$. With all these building blocks available, we can proceed to specific calculations.

However, before presenting the results, we must note an important feature which largely changes the view on the results of this section. It is easy to show that the diffusion problem we solve here is singular. Indeed, suppose in general that the driving field is composed of two parts, the first one being the drift due to an incompressible flow, and the second one being the conservative force originating from a fixed scalar potential. Then, if the streamlines of the flow are everywhere perpendicular to the conservative force, then there exists a stationary solution which depends only on the conservative force. Therefore, the flow can be completely ignored.

In our case the walls of the tube play the role of external potential, which is constant inside the tube. At walls, the gradient of the potential is perpendicular to the walls, elsewhere

it is zero. But next to the walls, pure hydrodynamic flow is perpendicular to the walls, hence the gradient of the potential is perpendicular to the flow. This leads to the conclusion that in the case of purely hydrodynamic drift, the stationary density is constant everywhere inside the tube. The exact solution of the problem is a uniform density.

Therefore, the ϵ expansion for the backward projected density (11) must sum to a constant, if correct. Here we shall interpret it as a test of reliability of the approximations based on truncation of the ϵ expansion. If the first-order approximation in ϵ yields a result which is closer to uniform density than the zeroth order, we can deduce that we are on a good track. We shall see in the next subsection that it is indeed so, and we shall also assess quantitatively how close we are to the known exact result.

2. Specific example

We shall use spatially periodic and mirror-symmetric modulation of the tube diameter. Specifically, we choose

$$h(x) = \frac{d}{2}(2 - a\cos\Omega x). \tag{45}$$

The parameter d sets the average diameter, a is the amplitude of variation, and Ω the spatial frequency of the modulation. So the spatial period is $L = 2\pi/\Omega$. With this choice of geometry, and using the flow described by the stream function (35), we obtain the following set of functions:

$$\begin{aligned} \zeta_2(x) = -\zeta_0(x) &= \frac{q}{2\pi}\frac{a\Omega\sin\Omega x}{2 - a\cos\Omega x}, \\ \eta_1(x) &= \frac{8q}{\pi}\frac{1}{d^2(2-\cos\Omega x)^2}, \\ \zeta_1(x) = \eta_0(x) &= 0. \end{aligned} \tag{46}$$

Using them, we can directly apply the formalism of the last subsection to obtain the functions $\gamma_0(x)$, $\gamma_1(x)$, and $Z_1(x)$ and the core of the backward projector $\omega_1^\sigma(x, r)$. Now we can proceed to calculation of the particle density.

We are interested in the stationary states with spatial period L. Let us find the projected density first. The general stationary solution (37) should obey $p_1(x) = p_1(x + L)$. This condition fixes the constant c. Moreover, we expect that the average density is such that there is one particle per period, i.e., $\int_0^L p_a(x)\,dx = 1$. This condition is used to fix the stationary current j. Finally, we obtain the solution (up to the first order in ϵ) in the form

$$p_1(x) = \frac{jA_1(x)}{1 - e^{-\tilde\gamma_1(L)+\tilde\gamma_1(0)}}\int_x^{x+L}\frac{dx'}{A_1(x')[1-\epsilon Z_1(x')]}, \tag{47}$$

where $\tilde\gamma_1(x) = \gamma_0(x) + \epsilon\gamma_1(x)$ and the stationary current is given as

$$j = \frac{1 - e^{-\tilde\gamma_1(L)+\tilde\gamma_1(0)}}{\int_0^L A_1(x)\int_x^{x+L}\{A_1(x')[1-\epsilon Z_1(x')]\}^{-1}\,dx'\,dx}. \tag{48}$$

Finally, let us write the formula for the backward projected density:

$$\begin{aligned} \rho_1(x, r) = j\,e^{-G_{00}(x,r)}\Bigg\{&\frac{1+\epsilon\omega_1^I(x,r)}{1-e^{-\tilde\gamma_1(L)+\tilde\gamma_1(0)}} \\ &\times\int_x^{x+L}\frac{e^{-\tilde\gamma_1(x')+\tilde\gamma_1(x)}}{A_{00}(x')[1-\epsilon Z_1(x')]}\,dx' \\ &-\frac{\epsilon\omega_1^{II}(x,r)}{A_{00}(x)[1-\epsilon Z_1(x)]}\Bigg\}. \end{aligned} \tag{49}$$

This result holds up to the first order in ϵ. For comparison, we shall also compute analogous results in the zeroth order in ϵ. We shall not list here explicitly the formulas, because they are obtained from (47), (48), and (49) just by setting $\epsilon = 0$. Spatial distribution of the particle current can be found from (49) using formula (31) for the axial component and formulas (33) and (34) for the radial component.

We show in Fig. 1 results of the calculation of density (indicated by shades) and current (indicated by streamlines and arrows). We can clearly see that the zeroth approximation exaggerates the influence of the varying tube diameter on the particle probability density. The radial component of the flow pushes the particle too much toward the axis, when the flow is convergent, and too much to the wall, when the flow is divergent. However, it is also clear that this artifact of the zeroth order is extensively corrected by the first order, where, on the contrary, the compensation seems again to be too strong and the positions of maxima and minima are swapped. It points to the necessity of taking the higher order corrections to converge to the constant density, which is possible in principle within our mapping procedure, but technically it is extremely difficult. So we end up at the first order and continue our analysis within the following consideration.

Deviations of the stationary density from constant are (mostly) of the opposite signs in the zeroth order and after the first-order correction, Figs. 1(a) and 1(b). For any tested parameters a and q, we could (heuristically) find an optimum value of $\epsilon \in (0, 1)$ minimizing these deviations [see Fig. 1(c)], calculated for $\epsilon = 0.7$ (ϵ could be understood as an adjustable parameter, capable of involving partially also the higher order corrections, if a proper condition is given; here it is the requirement of a constant stationary ρ). At least, we can consider the results obtained within the zeroth- and the first-order approximations as the lower and upper estimates of the exact values. In the next subsection we shall apply the method to nontrivial situations containing additional external fields, using mostly the zeroth- and first-order approximations as the lower and upper estimates of the correct results.

B. Flotation and centrifugation

Let us now investigate the influence of external conservative forces. Here we consider just two possibilities, a uniform axial force and a centrifugal force, which is always perpendicular to the axis and its modulus scales with the distance from the axis. It can be realized by putting the entire tube into rotation around its axis. While the centrifugal force comes

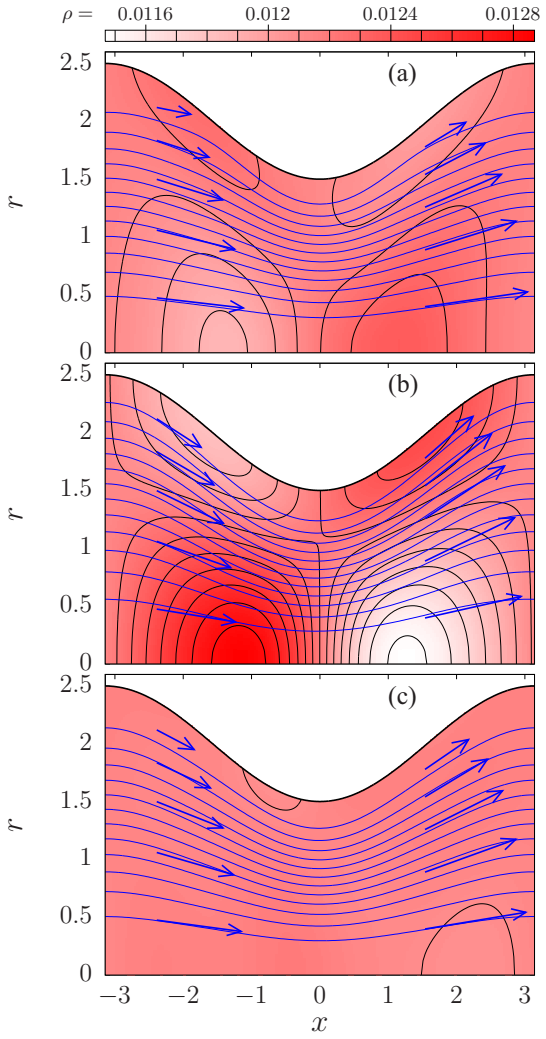

FIG. 1. Probability density for a particle carried by the flow in a tube with profile (45), where $\Omega = 1$, $d = 2$, and $a = 0.5$. The fluid flow is described by (35), where $q = 2$. (a) Backward projected density in an approximation up to the first order in ϵ, as given in (49). (b) The same in the zeroth order in ϵ. (c) The data for $\epsilon = 0.7$. The particle current is indicated by the streamlines, and it is also visualized by the arrows showing direction and size of the current. The darker shade means larger probability density, according to the legend shown on the top of the figure.

from buoyancy, i.e., from the difference in specific weight of the fluid and the material of the particles, the axial force can originate from two sources. The first option is gravity, i.e., buoyancy, as in the case of centrifugal force. It requires only making the tube axis vertical. The second option relies on endowing the particles with electrostatic charge and putting the apparatus in a uniform electric field oriented parallel to the axis. Anticipating the dependence on the size of the particles, we note that the forces originating from buoyancy scale with volume, i.e., the third power of the particle radius, while electrostatic force is independent of the radius. For simplicity, we shall use the term "flotation" for both mechanisms induced by axial force, while the term centrifugation obviously pertains to the centrifugal force.

So let us suppose that addition of the conservative forces changes the expression (36) to

$$\begin{aligned} g(x,r) &= -\frac{1}{r}\frac{\partial\psi(x,r)}{\partial x} + br, \\ f(x,r) &= \frac{1}{r}\frac{\partial\psi(x,r)}{\partial r} - f_0, \end{aligned} \tag{50}$$

where b and f_0 are the measures of the centrifugal and axial forces, respectively. Consequently, the functions (46) become

$$\begin{aligned} \zeta_2(x) &= \frac{q}{2\pi}\frac{a\Omega\sin\Omega x}{2-a\cos\Omega x}, \\ \zeta_1(x) &= \frac{b\,d^2}{8}(2-a\cos\Omega x)^2, \\ \zeta_0(x) &= -\frac{q}{2\pi}\frac{a\Omega\sin\Omega x}{2-a\cos\Omega x} - \frac{b\,d^2}{8}(2-a\cos\Omega x)^2, \\ \eta_1(x) &= \frac{8q}{\pi}\frac{1}{d^2(2-\cos\Omega x)^2}, \\ \eta_0(x) &= -f_0. \end{aligned} \tag{51}$$

This set of five functions serves as an input to the formalism developed in the last section. Therefore, we can directly calculate the particle density and current at each point of the tube. However, before we proceed to such a calculation, we must clarify the dependence of all processes involved on the size of the particles.

Introducing the forces f and g and scaling the time by D_0 in Sec. II A 1, we work in units of measurement where the diffusion coefficient $D_0 = k_BT/(6\pi\eta R)$ and mobility $\mu = 1/(6\pi\eta R)$ as well as the particle radius R are unity. We call these units the reduced units of measurement. This way the dependence on particle size is made implicit, because in units of measurement, where the length unit is fixed, the diffusion coefficient is inversely proportional to the particle radius. We shall return to explicit dependence on the particle radius using such units of measurements in which the fractions $k_BT/(6\pi\eta)$ and $\mu = 1/(6\pi\eta)$ are unity, and the unit of length is fixed by a reference particle radius R_0, chosen at will. In the rest of the article we shall call these units of measurement the physical units. Then we introduce the quantity $R_{\rm red} = R/R_0$, called the reduced particle radius. For $R_{\rm red} = 1$ both the diffusion coefficient and mobility are unity.

The volumetric flow Q and the current J expressed in physical units of measurement are related to corresponding quantities q and j expressed in the reduced units as

$$q = Q\,R_{\rm red}, \quad J = j/R_{\rm red}. \tag{52}$$

The conservative forces remain seemingly unaffected, because both diffusion coefficient and mobility scale equally with the particle size. However, we must take into account yet another source of particle size dependence. Indeed, the forces originating in buoyancy, i.e., the centrifugal force and the gravitational axial force, are proportional to the volume of the particle. Therefore, we must also replace

$$b = B\,R_{\rm red}^3, \quad f_0 = F_{0e} + F_{0g}\,R_{\rm red}^3, \tag{53}$$

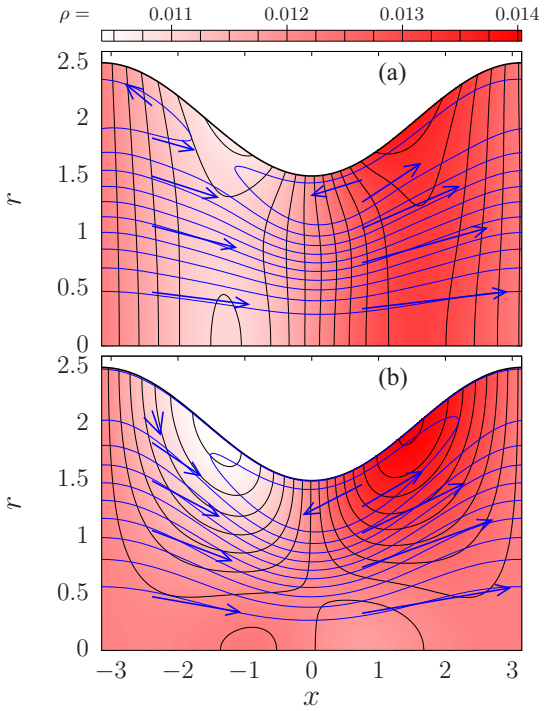

FIG. 2. Probability density for a particle carried by the flow in a tube with the same profile and fluid velocity as in Fig. 1 and $Q = 2$ calculated in the first (a) and the zeroth (b) order in ϵ. The particles are in an external axial electrostatic field with strength $F_{0e} = 0.2$. The reduced particle size is $R_{\text{red}} = 2$. Meaning of the symbols is the same as in Fig. 1.

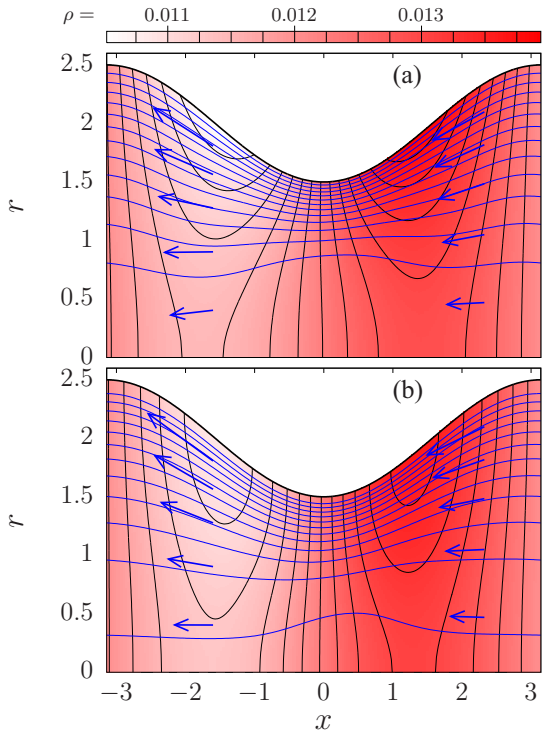

FIG. 3. Probability density for a particle carried by the flow in a tube with the same profile and fluid velocity as in Fig. 1 and $Q = 2$. The particles are in an external axial electrostatic field with strength $F_{0e} = 0.2$. The reduced particle size is $R_{\text{red}} = 0.5$. Meaning of the symbols is the same as in Fig. 1.

where F_{0e} measures the electrostatic and F_{0g} the gravitational component of the axial force in the physical units, while B measures the centrifugal force in the physical units.

Let us first look at the effect of flotation. We show in Figs. 2 and 3 particle density calculated in the zeroth (panels b) and the first-order (panels a) approximation in ϵ for axial force of electrostatic origin, i.e., not scaling with the size of the particle, $F_{0e} = 0.2$ and reduced particle sizes $R_{\text{red}} = 2$ and $R_{\text{red}} = 0.5$, respectively.

Generically, we observe that the role of the first correction in ϵ is less significant when conservative forces dominate. Here it is the case with $R_{\text{red}} = 0.5$ (Fig. 3), as can be clearly seen from the overwhelming flow of the particles to the left, despite the hydrodynamic drift, which tends to push the particles to the right. However, when the hydrodynamic forces are comparable, or even dominant to the conservative forces, inclusion of the first correction in ϵ is indispensable, as demonstrated in Fig. 2. On the one hand we can see that the competition of axial force with hydrodynamic drag results in a complicated pattern of the particle current, also containing vortices, and on the other hand, we can observe that the first correction in ϵ significantly changes the particle density.

Now let us turn to the effect of centrifugation. We show in Figs. 4 and 5 the particle density for $B = 0.2$ and the reduced particle sizes $R_{\text{red}} = 0.5$ and $R_{\text{red}} = 1.5$, respectively. We can observe how the centrifugal force concentrates the particles in the farthest periphery of the tube. This effect is stronger for larger particles, as buoyancy is proportional to volume of the particles. Comparing the results of the zeroth (panels b) and the first order (panels a) in ϵ, we come to the same conclusion as in the case of axial force, namely, that inclusion of the first correction is crucial when the conservative forces are comparable or weaker than the hydrodynamic drift. Contrary to the axial force, the particle current looks very simple, without any vortices. Indeed, there is no mechanism to create them, as long as there are no vortices in the flow of the fluid itself.

C. Particle separation

A microfluidic device can work as a particle separator if there is sufficiently strong dependence of its parameters on particle size. The mechanism we investigate here is analogous to chromatography, where each substance is carried by a moving phase at a specific velocity. In our case, we need that the average particle velocity be size-specific. In order to study our problem from this point of view, we calculate the total current, as given by (48). In fact, it is more practical to express the average particle velocity $\langle \dot{x} \rangle = 2\pi J/\Omega$ from it, because this quantity is independent of average particle density.

Let us first investigate flotation. We show in Fig. 6 the velocity of particles subject to gravity in a vertical tube. We assume that the flow of the carrying fluid goes upward, thus gravity acts against it. Therefore, particles can be separated according to which of the driving agents prevails. For very small particles, gravity is negligible, and the particle velocity is dictated only by the velocity of the fluid. On the contrary,

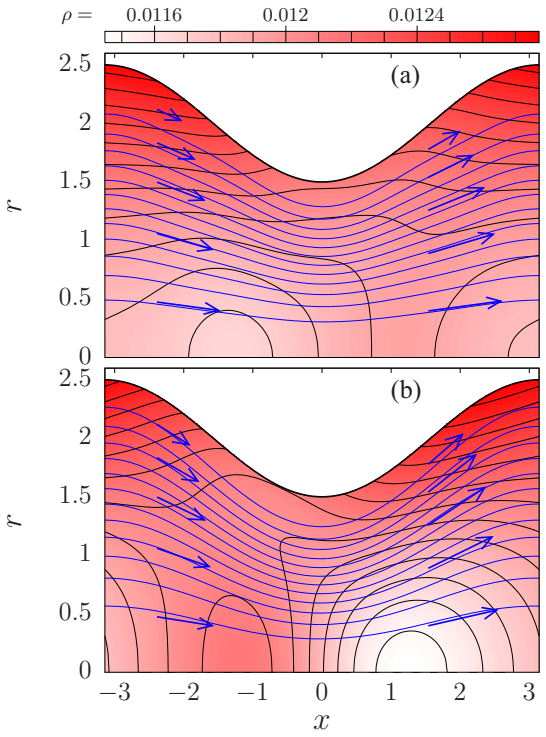

FIG. 4. Probability density for a particle carried by the flow in a tube with the same profile and fluid velocity as in Fig. 1 and $Q = 2$. The particles are subject to centrifugal force with strength $B = 0.2$. The reduced particle size is $R_{\rm red} = 0.5$. Meaning of the symbols is the same as in Fig. 1.

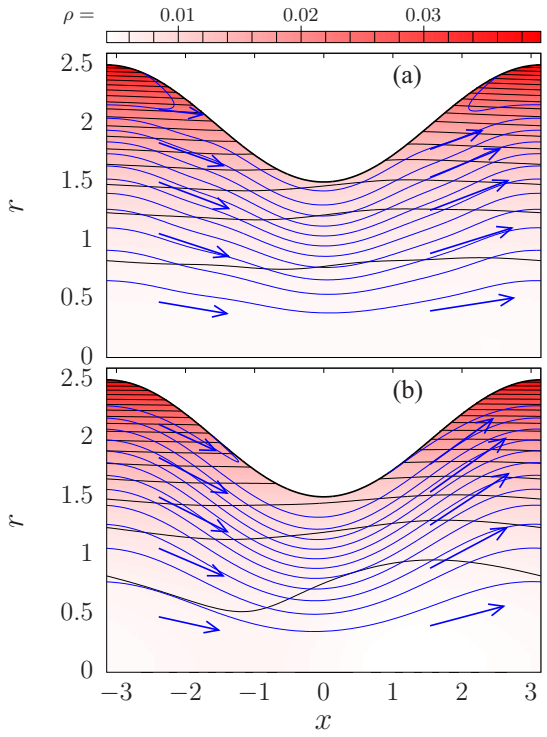

FIG. 5. Probability density for a particle carried by the flow in a tube with the same profile and fluid velocity as in Fig. 1 and $Q = 2$. The particles are subject to centrifugal force with strength $B = 0.2$. The reduced particle size is $R_{\rm red} = 1.5$. Meaning of the symbols is the same as in Fig. 1.

for large particles gravity is dominant and particles are pushed back down. We are not free to tune the parameter F_{0h}, which measures the buoyancy, but adjusting the fluid velocity (i.e., the parameter Q) we can sharply separate particles larger than prescribed $R_{\rm red}$ from smaller ones.

The separator based on electrostatic flotation is similar in principle; an external field pushes the particles against the flow. But in contrast to gravity, the force is independent of the particle size. This leads to the opposite trend in the size dependence, compared to gravity. Smaller particles have a larger diffusion constant and mobility, and therefore driving by external field prevails. On the contrary, larger particles are more attached to the fluid flow, and external field becomes negligible. In this case, we can tune both the strength of the external field and the velocity of the fluid. In this way we again adjust the critical $R_{\rm red}$ so that smaller particles will be pushed back and larger particles will be carried farther by the fluid. We show the dependence of the particle velocity on $R_{\rm red}$ in Fig. 7.

Separation by centrifugation works differently. The tube rotates around its axis, and particles are pushed toward the walls. In our geometry the diameter of the tube varies periodically, and the particles accumulate preferentially in the areas of larger diameter and they are wiped out from the central area where the flow has large velocity. This results in diminishing the total flow of particles. The separation capability is based on the fact that larger particles feel more strongly the centrifugal force. However, in contrast to flotation, the particle velocity is only slowed, rather than reverted, when the centrifugal force increases. We show in Fig. 8 dependence of the particle velocity on $R_{\rm red}$. For very small particles, the velocity corresponds to particles carried freely by the flow, as in the case of gravitational flotation.

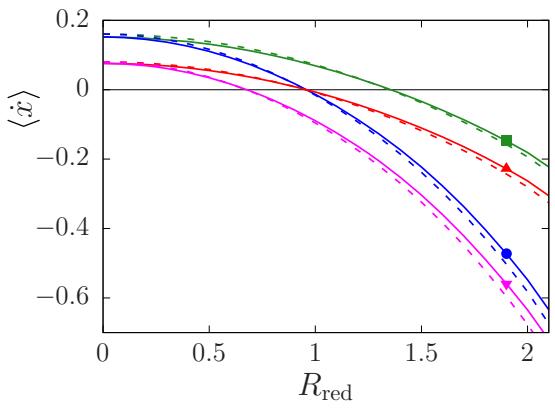

FIG. 6. Dependence of the average particle velocity on the reduced particle diameter. The tube has profile (45),where $\Omega = 1$, $d = 2$, and $a = 0.5$, and the fluid flow is described by (35) with $Q = 2$ (● and ■) and $Q = 1$ (▲ and ▼). The particles are subject to gravity in the axial direction, with $F_{0g} = 0.1$ (■ and ▲) and $F_{0g} = 0.2$ (● and ▼). The dashed lines here and in all following figures represent the zeroth-order approximation; the solid lines depict calculations up to the first order in ϵ.

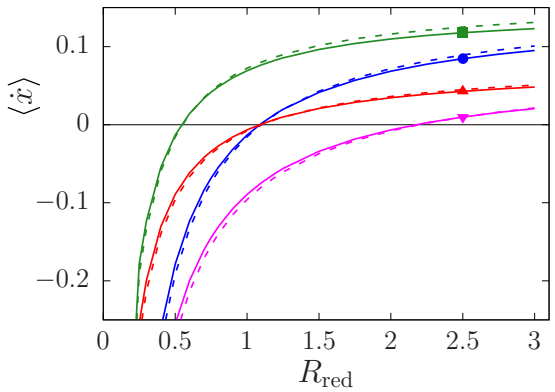

FIG. 7. Dependence of the average particle velocity on the reduced particle diameter. The tube has profile (45), where $\Omega = 1$, $d = 2$, and $a = 0.5$ and the fluid flow is described by (35) with $Q = 2$ (● and ■) and $Q = 1$ (▲ and ▼). The particles are subject to electrostatic force in the axial direction with $F_{0e} = 0.1$ (■ and ▲) and $F_{0e} = 0.2$ (● and ▼).

It seems that the best separations can be obtained by combination of flotation and centrifugation. We show in Fig. 9 how the average particle velocity depends on the particle radius, when the particles are subject to centrifugal and electrostatic force. By tuning the field and rotation speed we can adjust the maximum current at the preferred particle size.

Another interesting quantity which can influence separation of the particles is an effective diffusion constant D^*. The Reimann formula [92,93] is extended by including the spatial dependent effective diffusion coefficient $D(x)$ [50,94],

$$D^* = \frac{L^2 \int_0^L \frac{dx}{A(x)D(x)} \int_{x-L}^{x} \frac{dz}{A(z)D(z)} I^2(z)}{\left[\int_0^L \frac{dx}{A(x)D(x)} I(x)\right]^3}, \tag{54}$$

where

$$I(x) = \int_{x-L}^{x} A(y)\, dy \tag{55}$$

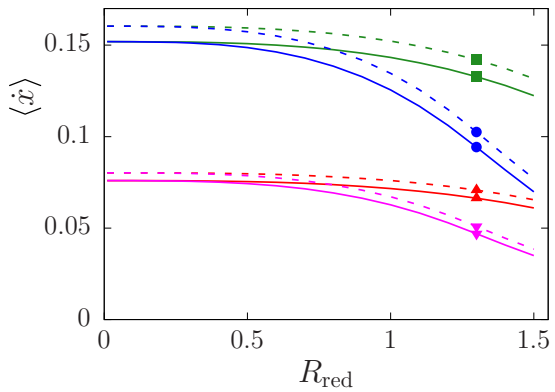

FIG. 8. Dependence of the average particle velocity on the reduced particle diameter. The tube has profile (45), where $\Omega = 1$, $d = 2$, and $a = 0.5$, and the fluid flow is described by (35) with $Q = 2$ (● and ■) and $Q = 1$ (▲ and ▼). The particles are subject to centrifugal force with $B = 0.1$ (■ and ▲) and $B = 0.3$ (● and ▼).

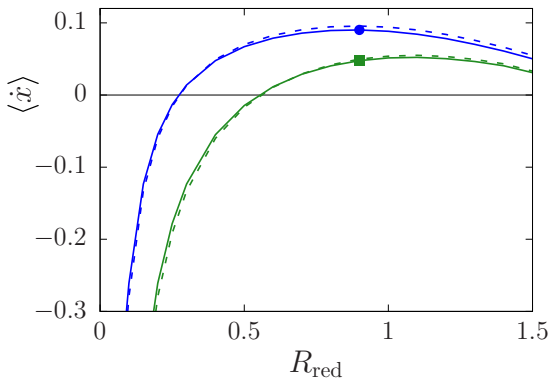

FIG. 9. Dependence of the average particle velocity on the reduced particle diameter. The tube has profile (45), where $\Omega = 1$, $d = 2$, and $a = 0.5$, and the fluid flow is described by (35) with $Q = 2$. The particles are subject to combined centrifugal force with $B = 0.3$ and electrostatic axial force with $F_{0e} = 0.1$ (■) and $F_{0e} = 0.05$ (●).

integrates properties of a periodic channel given by its corrugation over one period L and characterizes diffusion on a much larger scale than L. In our case, $A(x) = A_0(x)$ and $D(x) = 1$ in the zeroth-order approximation, while $A(x) = A_1(x)$ and $D(x) = 1 - \epsilon Z_1(x)$ after also taking the first-order correction.

We present the effective coefficient D^* depending on the axial force f_0 for several values of q in Fig. 10 for two

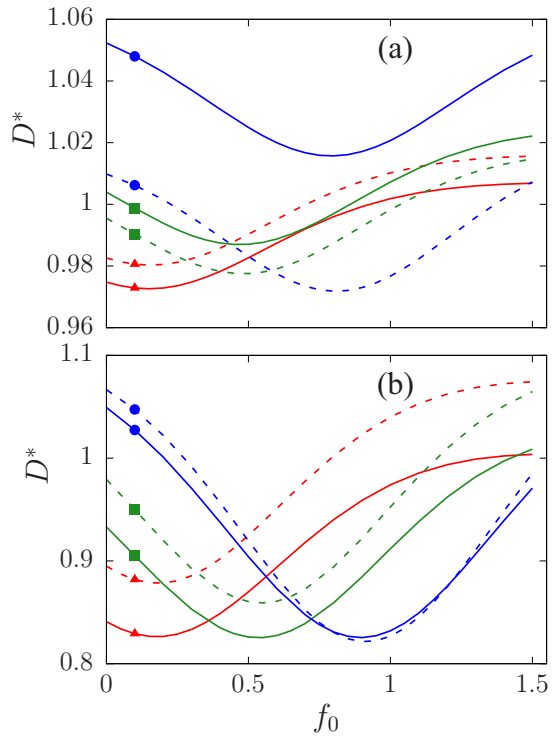

FIG. 10. Dependence of the effective diffusion constant on the axial force. The tube has profile (45), where $\Omega = 1$; $d = 2$; $a = 0.2$ (a) and $a = 0.5$ (b). The fluid flow is described by (35) with $q = 2$ (▲), $q = 6$ (■), $q = 10$ (●). The dashed lines are results of the zeroth-approximation in ϵ, and the full lines include the first-order correction in ϵ.

amplitudes of corrugation, $a = 0.2$ (upper panel) and $a = 0.5$ (lower panel). The data are calculated within the zeroth-order approximation (dashed lines) and including the first-order correction (solid lines); these lines are supposed to determine the upper and lower estimates for the exact results. The typical behavior of all curves exhibits a minimum at the force corresponding to changing direction of the averaged velocity. It can be explained by Fig. 2, which depicts the density and fluxes for such parameters. The particles are partially trapped in whirls at the bottlenecks, which can slow the diffusion on a large scale. It is an effect of corrugation of the tube; the minimum of D^* for larger amplitude a is more distinctive.

The values of D^* for the first-order approximation in the limit $q \to 0$ and $f_0 \to 0$ are well approximated by the formula of Reguera *et al.* [50], giving $D^* = 0.970575$ or 0.832722 for $a = 0.2$ and 0.5, respectively. The zeroth-order D^* approaches the values 0.980137 and 0.880224, respectively, calculated for the FJ approximation. The first-order corrections due to corrugation decrease the diffusion coefficient $D(x)(< D_0)$, as well as the effective D^*, which can be seen in Fig. 10(b) for $a = 0.5$, $q = 2$ and 6. On the other hand, the presence of the flux increases the diffusion coefficient $D(x) = 1 - Z_1(x) \simeq 1 + q^2/[48\pi^2 h^2(x)] > 1$, if approximated by the leading terms [77]. The other terms included in our first-order correction Z_1 even raise the resultant D^* above the zeroth order, as seen in Fig. 10(a) for $a = 0.2$, when the corrugation is small and does not play an important role.

Nevertheless, both our approximations demonstrate that unlike the diffusion in a flat tube, where the separation is based on changing direction of the net flux, there is a specific regime in corrugated channels near the critical force f_0 when the particles are trapped and their effective dispersion is minimized.

IV. CONCLUSIONS

The systematic procedure of mapping of 3D diffusion problems with general, conservative as well as nonconservative driving on an effective 1D diffusion problem was presented here. It summarizes and generalizes development obtained earlier for 2D geometry. We showed that in the presence of nonconservative forces, like the hydrodynamic drift, the lowest order approximation may not be satisfactory, and calculation of the higher order corrections enabled by our theory can improve reliability of the obtained results.

We applied the mapping procedure to diffusion of particles driven primarily by the hydrodynamic flow. Because of the complexity of the calculations, we restricted ourselves only up to the first-order approximation. The stationary density in the pure hydrodynamic driving represents a good test of our calculations; the exact solution is a constant. As the deviations of the zeroth-order and the first-order approximations from the constant have opposite signs, we consider the results of both approximations as the upper and the lower estimates of the exact values.

For construction of particle separation devices, the hydrodynamic drift has to be combined with other (conservative) forces. We considered two of them, a constant force acting along the axis (e.g., gravitation, flotation) and the centrifugal force, when the tube rotates around its axis. For a fixed hydrodynamic flow and growing axial force, the resultant direction of the net flow of particles depends on their properties, e.g., the size, as expected.

By tuning the volumetric flow of the fluid and the external conservative fields we can adjust the critical particle size so that particles larger than critical go in the opposite direction than the particles smaller than critical. In this setting, we closely observe the regime in which the competing forces are almost equal and the net particle current approaches zero, i.e., around the critical particle size. In order to achieve as clean a separation as possible, it is beneficial to have a low diffusion coefficient. This is exactly what we observe; near the regime of a zero particle current the effective diffusion coefficient D^* has a minimum. Its origin comes from the fact that the particles are partially trapped, circulating in whirls near the bottlenecks of the tube.

Correspondingly, one of the most important findings is that the minimum of the effective diffusion constant becomes more distinctive when the amplitude of corrugation of the tube increases. This suggests that separation in corrugated tubes might be more accurate than in the straight ones.

Besides that, the centrifugation separation technique based on axial rotation of the tube relies entirely on the corrugation of the tube. Larger particles feel larger centrifugal forces and are trapped in corrugation "pockets," while small particles are carried more freely by the flow. This suggests the application as a cleaning device. However, the combination of centrifugal and axial force leads again to a competition, which results in a maximum in the dependence of the particle current on particle radius. This means that in such a combined setup movement of particles of specific size is preferred. This may serve as a kind of chromatographic particle separator. The corrugation of the tube is an essential component here, as the separation effect of a centrifugal force is neutral in a straight tube. The current technology of polydimethylsiloxane molding (see, e.g., Ref. [14]) allows routine fabrication of nearly any shape of such corrugation on the scale of several micrometers, with submicrometer precision.

Generally speaking, an open question remains, namely, whether the series in ϵ could be partially resummed, as was done in Ref. [65]. This would result in a formula for an effective position-dependent diffusion coefficient. For now, technical difficulties hinder the progress in this direction. We tried to emulate the resummation by adjusting the value of ϵ by hand, which was rather successful, but this procedure is too crude and not well controlled to be reliable in a generic situation. Therefore, we leave the problem of resummation of the ϵ series for future consideration.

An open problem of great practical importance is the influence of hydrodynamic particle-particle interactions in dense colloidal suspensions. Such interactions can have a large positive impact on particle transport, as demonstrated experimentally in a recent work [95]. If such transport occurs in channels of variable diameter, hydrodynamic interactions bring further complexity. Mapping such systems on an effective 1D problem is a challenge requiring substantially new ideas, and this is the direction of future research.

ACKNOWLEDGMENT

The work was supported by the Grant Agency of the Czech Republic, Grant No. 17-06716S and the Slovak VEGA Grant No. 2/0008/18.

APPENDIX

1. Functions $\zeta_\alpha(x)$ and $\eta_\alpha(x)$

For pure hydrodynamic driving defined by (35) and (36) we have

$$\zeta_0(x) = -\frac{Q\,h'(x)}{2\pi h(x)}, \quad \zeta_1(x) = 0, \quad \zeta_2(x) = \frac{Q\,h'(x)}{2\pi h(x)}, \quad \eta_0(x) = 0, \quad \eta_1(x) = \frac{2Q}{\pi h^2(x)}. \tag{A1}$$

In more complicated cases, the functions $\zeta_1(x)$ and $\eta_0(x)$ may not be zero.

2. Functions $T^I_{1,\alpha}(x)$ and $T^{II}_{1,\alpha}(x)$

The set of functions T^I and T^{II} is

$$\begin{aligned}
T^I_0(x) &= \widetilde{\zeta'_2(x)}^2\langle v^4\rangle(x) + [2\widetilde{\zeta'_1(x)}\widetilde{\zeta'_2(x)} + +\eta_1(x)\widetilde{\zeta'_2(x)}]\langle v^3\rangle(x)\\
&\quad + \left[-\widetilde{\zeta''_2(x)} + \widetilde{\zeta'_1(x)}^2 + 2\widetilde{\zeta'_0(x)}\widetilde{\zeta'_2(x)} + \eta_0(x)\widetilde{\zeta'_2(x)} + \eta_1(x)\widetilde{\zeta'_1(x)} + \widetilde{\zeta'_2(x)}\frac{2h'(x)}{h(x)\Lambda(x)}\right]\langle v^2\rangle(x)\\
&\quad + \left\{-\widetilde{\zeta''_1(x)} - \widetilde{\eta'_1(x)} + 2\widetilde{\zeta'_0(x)}\widetilde{\zeta'_1(x)} + \eta_0(x)\widetilde{\zeta'_1(x)} + \eta_1(x)\widetilde{\zeta'_0(x)} + [\widetilde{\zeta'_1(x)} + \eta_1(x)]\frac{2h'(x)}{h(x)\Lambda(x)}\right\}\langle v\rangle(x)\\
&\quad - [2\widetilde{\zeta'_1(x)}\langle v\rangle(x) + 2\widetilde{\zeta'_2(x)}\langle v^2\rangle(x) + \eta_1(x)\langle v\rangle(x)]\{\widetilde{\zeta'_0(x)} + \eta_0(x) + [\widetilde{\zeta'_1(x)} + \eta_1(x)]\langle v\rangle(x) + \widetilde{\zeta'_2(x)}\langle v^2\rangle(x)\},\\
T^I_1(x) &= \widetilde{\zeta''_1(x)} + \widetilde{\eta'_1(x)} - 2\widetilde{\zeta'_0(x)}\widetilde{\zeta'_1(x)} - \eta_1(x)\widetilde{\zeta'_0(x)} - \eta_0(x)\widetilde{\zeta'_1(x)} + [2\widetilde{\zeta'_1(x)} + \eta_1(x)]\{\widetilde{\zeta'_0(x)} + \eta_0(x) + [\widetilde{\zeta'_1(x)} + \eta_1(x)]\langle v\rangle(x)\\
&\quad + \widetilde{\zeta'_2(x)}\langle v^2\rangle(x)\},\\
T^I_2(x) &= \widetilde{\zeta''_2(x)} - \widetilde{\zeta'_1(x)}^2 - 2\widetilde{\zeta'_0(x)}\widetilde{\zeta'_2(x)} - \eta_1(x)\widetilde{\zeta'_1(x)} - \eta_0(x)\widetilde{\zeta'_2(x)} + 2\widetilde{\zeta'_2(x)}\{\widetilde{\zeta'_0(x)} + \eta_0(x) + [\widetilde{\zeta'_1(x)} + \eta_1(x)]\langle v\rangle(x)\\
&\quad + \widetilde{\zeta'_2(x)}\langle v^2\rangle(x)\},\\
T^I_3(x) &= -2\widetilde{\zeta'_1(x)}\widetilde{\zeta'_2(x)} - \eta_1(x)\widetilde{\zeta'_2(x)},\\
T^I_4(x) &= -\widetilde{\zeta'_2(x)}^2,\\
T^{II}_0(x) &= \frac{2h'(x)}{h(x)\Lambda(x)} - [2\widetilde{\zeta'_1(x)} + \eta_1(x)]\langle v\rangle(x) - 2\widetilde{\zeta'_2(x)}\langle v^2\rangle(x),\\
T^{II}_1(x) &= 2\widetilde{\zeta'_1(x)} + \eta_1(x),\\
T^{II}_2(x) &= 2\widetilde{\zeta'_2(x)}.
\end{aligned} \tag{A2}$$

In these formulas we defined the following combinations:

$$\begin{aligned}
\widetilde{\eta'_0(x)} &= \eta'_0(x) + \frac{2h'(x)}{h(x)}\eta_1(x),\\
\widetilde{\eta'_1(x)} &= \eta'_1(x) - \frac{2h'(x)}{h(x)}\eta_1(x),\\
\widetilde{\zeta'_0(x)} &= \zeta'_0(x) + \frac{2h'(x)}{h(x)}\zeta_1(x),\\
\widetilde{\zeta'_1(x)} &= \zeta'_1(x) - \frac{2h'(x)}{h(x)}\zeta_1(x) + \frac{4h'(x)}{h(x)}\zeta_2(x),\\
\widetilde{\zeta'_2(x)} &= \zeta'_2(x) - \frac{4h'(x)}{h(x)}\zeta_2(x),\\
\widetilde{\zeta''_0(x)} &= \zeta''_0(x) + \frac{2h''(x)}{h(x)}\zeta_1(x) + \frac{4h'(x)}{h(x)}\zeta'_1(x) - \frac{6h'^2(x)}{h^2(x)}\zeta_1(x) + \frac{8h'^2(x)}{h^2(x)}\zeta_2(x),
\end{aligned}$$

$$\widetilde{\zeta_1''(x)} = \zeta_1''(x) - \frac{2h''(x)}{h(x)}\zeta_1(x) - \frac{4h'(x)}{h(x)}\zeta_1'(x) + \frac{6h'^2(x)}{h^2(x)}\zeta_1(x) - \frac{28h'^2(x)}{h^2(x)}\zeta_2(x) + \frac{8h'(x)}{h(x)}\zeta_2'(x) + \frac{4h''(x)}{h(x)}\zeta_2(x),$$
$$\widetilde{\zeta_2''(x)} = \zeta_2''(x) - \frac{2h''(x)}{h(x)}\zeta_1(x) + \frac{20h'^2(x)}{h^2(x)}\zeta_2(x) - \frac{8h'(x)}{h(x)}\zeta_2'(x) - \frac{4h''(x)}{h(x)}\zeta_2(x). \tag{A3}$$

3. Expressions for $\langle v^k \rangle$

Of course, $\langle v^0 \rangle = 1$. For the first power we have

$$\langle v \rangle(z_1, z_2) = -\frac{z_1}{2z_2} + \frac{1}{2z_2\Lambda(z_1, z_2)} - \frac{e^{-z_1-z_2}}{2z_2\Lambda(z_1, z_2)}, \tag{A4}$$

and the recurrence formula

$$\langle v^k \rangle(z_1, z_2) = -\frac{z_1}{2z_2}\langle v^{k-1} \rangle(z_1, z_2) + \frac{k-1}{2z_2\Lambda(z_1, z_2)}\langle v^{k-2} \rangle(z_1, z_2) - \frac{e^{-z_1-z_2}}{2z_2\Lambda(z_1, z_2)} \tag{A5}$$

allows calculation of all higher powers.

[1] X. Xuan, J. Zhu, and C. Church, Microfl. Nanofl. **9**, 1 (2010).
[2] T. P. Lagus and J. F. Edd, J. Phys. D: Appl. Phys. **46**, 114005 (2013).
[3] P. Sajeesh and A. K. Sen, Microfluidics Nanofluidics **17**, 1 (2014).
[4] J. Xuan and M. L. Lee, Anal. Methods **6**, 27 (2014).
[5] H. Amini, W. Lee, and D. Di Carlo, Lab Chip **14**, 2739 (2014).
[6] T. Salafi, K. K. Zeming, and Y. Zhang, Lab Chip **17**, 11 (2017).
[7] G. M. Whitesides, Nature (London) **442**, 368 (2006).
[8] T. M. Squires and S. R. Quake, Rev. Mod. Phys. **77**, 977 (2005).
[9] P. Huber, J. Phys.: Condens. Matter **27**, 103102 (2015).
[10] S. Kim and S. J. Karilla, *Microhydrodynamics* (Dover Publications, New York, 2005).
[11] G. Segré and A. Silberberg, J. Fluid Mech. **14**, 136 (1962).
[12] J. P. Matas, J. F. Morris, and E. Guazzelli, Oil Gas Sci. Technol. **59**, 59 (2004).
[13] E. S. Asmolov, Phys. Fluids **14**, 15 (2002).
[14] D. Di Carlo, D. Irimia, R. G. Tompkins, and M. Toner, Proc. Natl. Acad. Sci. USA **104**, 18892 (2007).
[15] J. Seo, M. H. Lean, and A. Kole, Appl. Phys. Lett. **91**, 033901 (2007).
[16] A. A. S. Bhagat, S. S. Kuntaegowdanahalli, and I. Papautsky, Phys. Fluids **20**, 101702 (2008).
[17] A. A. S. Bhagat, H. Bow, H. W. Hou, S. J. Tan, J. Han, and C. T. Lim, Med. Biol. Eng. Comput. **48**, 999 (2010).
[18] M. Masaeli, E. Sollier, H. Amini, W. Mao, K. Camacho, N. Doshi, S. Mitragotri, A. Alexeev, and D. Di Carlo, Phys. Rev. X **2**, 031017 (2012).
[19] J. M. Martel and M. Toner, Sci. Rep. **3**, 3340 (2013).
[20] J. Zhou and I. Papautsky, Lab Chip **13**, 1121 (2013).
[21] M. G. Lee, S. Choi, H.-J. Kim, H. K. Lim, J.-H. Kim, N. Huh, and J.-K. Park, Appl. Phys. Lett. **98**, 253702 (2011).
[22] M. G. Lee, S. Choi, and J. K. Park, J. Chromatogr. A **1218**, 4138 (2011).
[23] J. Zhang, M. Li, W. Li, and G. Alici, J. Micromech. Microeng. **23**, 085023 (2013).
[24] F. Slanina, Phys. Rev. E **94**, 042610 (2016).
[25] F. Slanina, Phys. Rev. E **99**, 012604 (2019).
[26] K. Loutherback, J. Puchalla, R. H. Austin, and J. C. Sturm, Phys. Rev. Lett. **102**, 045301 (2009).
[27] L. R. Huang, E. C. Cox, R. H. Austin, and J. C. Sturm, Science **304**, 987 (2004).
[28] M. P. MacDonald, G. C. Spalding, and K. Dholakia, Nature (London) **426**, 421 (2003).
[29] F. Petersson, L. Åberg, A.-M. Swärd-Nilsson, and T. Laurell, Anal. Chem. **79**, 5117 (2007).
[30] S. Matthias and F. Müller, Nature (London) **424**, 53 (2003).
[31] C. Kettner, P. Reimann, P. Hänggi, and F. Müller, Phys. Rev. E **61**, 312 (2000).
[32] K. Mathwig, F. Müller, and U. Gösele, New J. Phys. **13**, 033038 (2011).
[33] M. J. Skaug, C. Schwemmer, S. Fringes, C. D. Rawlings, and A. W. Knoll, Science **359**, 1505 (2018).
[34] P. Reimann, Phys. Rep. **361**, 57 (2002).
[35] P. Hänggi, F. Marchesoni, and F. Nori, Ann. Phys. (Leipzig) **14**, 51 (2005).
[36] P. Hänggi and F. Marchesoni, Rev. Mod. Phys. **81**, 387 (2009).
[37] C. Marquet, A. Buguin, L. Talini, and P. Silberzan, Phys. Rev. Lett. **88**, 168301 (2002).
[38] P. S. Burada, G. Schmid, P. Talkner, P. Hänggi, D. Reguera, and J. M. Rubí, Biosystems **93**, 16 (2008).
[39] P. S. Burada, P. Hänggi, F. Marchesoni, G. Schmid, and P. Talkner, Chem. Phys. Chem. **10**, 45 (2009).
[40] D. Reguera, A. Luque, P. S. Burada, G. Schmid, J. M. Rubí, and P. Hänggi, Phys. Rev. Lett. **108**, 020604 (2012).
[41] T. Motz, G. Schmid, P. Hänggi, D. Reguera, and J. M. Rubí, J. Chem. Phys. **141**, 074104 (2014).
[42] S. Martens, A. V. Straube, G. Schmid, L. Schimansky-Geier, and P. Hänggi, Phys. Rev. Lett. **110**, 010601 (2013).
[43] S. Martens, G. Schmid, A. V. Straube, L. Schimansky-Geier, and P. Hänggi, Eur. Phys. J. Spec. Topics **222**, 2453 (2013).
[44] M. H. Jacobs, *Diffusion Processes* (Springer, New York, 1967).
[45] R. Zwanzig, J. Phys. Chem. **96**, 3926 (1992).
[46] D. Reguera and J. M. Rubí, Phys. Rev. E **64**, 061106 (2001).
[47] A. Berezhkovskii and A. Szabo, J. Chem. Phys. **135**, 074108 (2011).
[48] P. Kalinay and J. K. Percus, J. Chem. Phys. **122**, 204701 (2005).
[49] P. Kalinay and J. K. Percus, Phys. Rev. E **72**, 061203 (2005).
[50] D. Reguera, G. Schmid, P. S. Burada, J. M. Rubí, P. Reimann, and P. Hänggi, Phys. Rev. Lett. **96**, 130603 (2006).

[51] P. S. Burada, G. Schmid, D. Reguera, J. M. Rubí, and P. Hänggi, Phys. Rev. E **75**, 051111 (2007).
[52] A. M. Berezhkovskii, M. A. Pustovoit, and S. M. Bezrukov, J. Chem. Phys. **126**, 134706 (2007).
[53] N. Laachi, M. Kenward, E. Yariv, and K. D. Dorfman, Europhys. Lett. **80**, 50009 (2007).
[54] I. D. Kosińska, I. Goychuk, M. Kostur, G. Schmid, and P. Hänggi, Phys. Rev. E **77**, 031131 (2008).
[55] R. M. Bradley, Phys. Rev. E **80**, 061142 (2009).
[56] A. Ryabov, V. Holubec, M. H. Yaghoubi, M. Varga, M. E. Foulaadvand, and P. Chvosta, J. Stat. Mech. (2016) 093202.
[57] V. Holubec, A. Ryabov, M. H. Yaghoubi, M. Varga, A. Khodaee, M. E. Foulaadvand, and P. Chvosta, Entropy **19**, 119 (2017).
[58] M. Mangeat, T. Guérin, and D. S. Dean, J. Stat. Mech. (2017) 123205.
[59] M. Mangeat, T. Guérin, and D. S. Dean, Europhys. Lett. **118**, 40004 (2017).
[60] N. Ogawa, Phys. Lett. A **377**, 2465 (2013).
[61] A. A. García-Chung, G. Chacón-Acosta, and L. Dagdug, J. Chem. Phys. **142**, 064105 (2015).
[62] L. Dagdug, A. A. García-Chung, and G. Chacón-Acosta, J. Chem. Phys. **145**, 074105 (2016).
[63] Y. Chávez, G. Chacón-Acosta, and L. Dagdug, J. Phys.: Condens. Matter **30**, 194001 (2018).
[64] P. Kalinay and J. K. Percus, J. Stat. Phys. **123**, 1059 (2006).
[65] P. Kalinay and J. K. Percus, Phys. Rev. E **74**, 041203 (2006).
[66] P. Kalinay and J. K. Percus, Phys. Rev. E **78**, 021103 (2008).
[67] P. Kalinay, Phys. Rev. E **94**, 012102 (2016).
[68] P. Kalinay, Phys. Rev. E **80**, 031106 (2009).
[69] W. Riefler, G. Schmid, P. S. Burada, and P. Hänggi, J. Phys.: Condens. Matter **22**, 454109 (2010).
[70] S. Martens, G. Schmid, L. Schimansky-Geier, and P. Hänggi, Phys. Rev. E **83**, 051135 (2011).
[71] S. Martens, G. Schmid, L. Schimansky-Geier, and P. Hänggi, Chaos **21**, 047518 (2011).
[72] P. Kalinay, Phys. Rev. E **84**, 011118 (2011).
[73] P. Kalinay and J. K. Percus, Phys. Rev. E **83**, 031109 (2011).
[74] P. Kalinay, Phys. Rev. E **89**, 042123 (2014).
[75] G. Taylor, Proc. R. Soc. London A **223**, 446 (1954).
[76] R. Aris, Proc. R. Soc. London A **235**, 67 (1956).
[77] S. Marbach and K. Alim, arXiv:1901.03697.
[78] B. Q. Ai, Y. F. He, F. G. Li, and W. R. Zhong, J. Chem. Phys. **138**, 154107 (2013).
[79] X. Yang, C. Liu, Y. Li, F. Marchesoni, P. Hänggi, and H. P. Zhang, Proc. Natl. Acad. Sci. USA **114**, 9564 (2017).
[80] P. Kalinay and F. Slanina, Phys. Rev. E **98**, 042141 (2018).
[81] P. Kalinay and F. Slanina, J. Phys.: Condens. Matter **30**, 244002 (2018).
[82] D. Bolster, M. Dentz, and T. Le Borgne, Phys. Fluids **21**, 056601 (2009).
[83] H. Blasius, Zs. Math. Phys. **58**, 225 (1910).
[84] J. A. Deiber and W. R. Schowalter, AIChE J. **25**, 638 (1979).
[85] J. M. Floryan, J. Fluid Mech. **482**, 17 (2003).
[86] S. A. Loh and H. M. Blackburn, Phys. Fluids **23**, 111703 (2011).
[87] H. K. Moffatt, J. Fluid Mech. **18**, 1 (1964).
[88] C. Pozrikidis, J. Fluid Mech. **180**, 495 (1987).
[89] N. Islam, B. H. Bradshaw-Hajek, S. J. Miklavcic, and L. R. White, Eur. J. Mech. B **53**, 119 (2015).
[90] M. Van Dyke, Adv. Appl. Mech. **25**, 1 (1987).
[91] P. K. Kitanidis and B. B. Dykaar, Transp. Porous Media **26**, 89 (1997).
[92] P. Reimann, C. Van den Broeck, H. Linke, P. Hänggi, J. M. Rubì, and A. Pérez-Madrid, Phys. Rev. E **65**, 031104 (2002).
[93] P. Reimann, C. Van den Broeck, H. Linke, P. Hänggi, J. M. Rubi, and A. Pérez-Madrid, Phys. Rev. Lett. **87**, 010602 (2001).
[94] P. Kalinay, J. Chem. Phys. **142**, 014106 (2015).
[95] K. Misiunas and U. F. Keyser, Phys. Rev. Lett. **122**, 214501 (2019).